Journal of
Engineering Sciences
Faculty of Engineering
Assiut University
JES
مجلة
العلوم الهندسية
كلية الهندسة
جامعة أسيوط
journal homepage: http://jesaun.journals.ekb.eg

Multi-objective optimal performance of a distribution system based on integrating renewable energy sources and hybrid energy systems

Received 14 February 2025; Revised 14 May 2025; Accepted 14 May 2025

Mahmoud El-Ghazaly [1]
Mazen Abdel-Salam [2]
Mohamed Nayel [3]
Mohamed Hashem [4]

Keywords
Distribution network performance,
Renewable energy sources,
Gravity,
Supercapacitor.

Abstract: Increasing integration of intermittent highly penetrated renewable energy sources (RESs) into electric distribution network (DN), coupled with variable load demands, introduces significant operational challenges related to voltage deviation, voltage stability, and power losses. To address these issues, this study proposes a new methodology for optimal integration of RESs, specifically photovoltaic (PV) and wind turbine (WT) generation, alongside hybrid energy storage systems (HESS) within the DN based on a recently developed Artificial Protozoa Optimizer (APO). The HESS employs a combination of long-duration gravity energy-storage (GES) and short-duration supercapacitor (SC) energy-storage. This method simultaneously optimizes allocation and operation of these components to minimize voltage deviations and power losses while enhancing voltage stability. The approach is validated and tested on the IEEE 33-bus DN, using a voltage-dependent time-varying mixed load model and variable solar irradiance wind speed. Results demonstrate that the combined deployment of RES and HESS can effectively minimize power loss by 46.1 % and voltage deviation by 64.7 %, as well as improve voltage stability by 7.42 %, leading to a significant enhancement of DN performance.

1. Introduction

1.1 Motivation and incitement

The increasing integration of PV and wind WT into electric DNs represents a crucial shift in global energy production, aimed at curtailing reliance on fossil fuels and mitigating associated carbon emissions. However, this proliferation of intermittent RESs, coupled with fluctuating load demands, introduces significant challenges. Consequently, the deployment of HESS, combining the strengths of multiple storage technologies including GES [1] and SC [2], has emerged as a critical necessity. Furthermore, the precise determination of the optimal

[1] Electrical Engineering Dept., Faculty of Engineering, Assiut University, Assiut, Egypt. mahmoudelghazaly@aun.edu.eg
[2] Electrical Engineering Dept., Faculty of Engineering, Assiut University, Assiut, Egypt. mazen@aun.edu.eg
[3] Electrical Engineering Dept., Faculty of Engineering, Assiut University, Assiut, Egypt. mohamed.nayel@aun.edu.eg
[4] Electrical Engineering Dept., Faculty of Engineering, Assiut University, Assiut, Egypt. mohamed.hashem575@eng.aun.edu.eg

https://doi.org/10.21608/jesaun.2025.360711.1426

allocation of RESs and HESS, is vital to achieve the desired performance enhancement of electric DNs [1].

1.2 Literature review

Numerous studies were conducted on the use of HESS to improve the stability of DNs with one or multiple buses. The current study aims to increase the stability of IEEE 33 bus DN combined with RESs by implementing a unique HESS that combines GES and SC. For this reason, the literature review focuses on studies investigating the use of HESS to enhance voltage stability in multi-bus DNs.

A study was reported on the optimal allocation of HESS including GES and SC in the IEEE 33-bus DN containing PV and WT using a proposed multi-objective PSO algorithm based on multi-strategy improvements [3] to minimize lifecycle cost, voltage deviation, and active power loss. Compared to the system without energy storage, the optimized configuration increased the minimum bus voltages by approximately 0.02-0.04 p.u. and reduced the peak active power loss by approximately 0.07 MW.

A study investigated a two-stage optimization for automated DN self-healing on the modified IEEE-69 bus DN using HESS including BES, HES, along with EV batteries [4]. In the first stage, the DN tried to recover the disconnected loads after identifying the fault and isolating the connected loads. This was made by doing feeder reconfiguration. In the second stage, announced loads are requested to reduce their value according to the level of their priority. Results showed that the presence of the HESS reduced load shedding by 7.86% and operation cost by 3.77% compared to the case without storage.

A study [5] was aimed at investigating a novel stochastic multistage dispatching model for minimizing three-phase unbalance on the modified IEEE 34-bus system, using a HESS including BES, EVs, and SC. Results showed that incorporating SC reduced real-time power unbalance by 3.27% and total operation cost by 46.77 $/day compared to the case without SC. On considering the cost of HESS degradation, the daily power imbalance dropped by 3.62 compared to the situation without SC.

A study [6] improved energy efficiency for a DN using HESS including thermal storage, BES, and SC, alongside PV, solar thermal collectors, and an internal combustion (diesel engine). The study considered uncertainties related to the PV and HESS, as well as demand-side management as indices. A horse herd optimization method was used for optimal allocation and operating of PV and HESS to minimize the use of fossil sources. Results showed that this optimized system reduced the use of fossil sources by almost 54.8%.

Selection of the optimum location, sizing, and power factors of biomass-based distributed generators (BDGs) in IEEE 69-bus and 33-bus DNs was investigated [7] using the Capuchin Search Algorithm. The study focuses on minimizing active power losses (PLI) while keeping branch current, bus voltage, and power flow constraints within acceptable limits.

An optimal allocation of PV panels and WTs as well as electric vehicle charging stations were investigated in the IEEE 118 and 33-bus DNs [8]. The results demonstrate significant improvements in DNs performance, achieving a reduction of 27.2% in PLI and a reduction of 79.5% in voltage deviation index (VDI) on the IEEE 33-bus DN, and a 34.2% reduction in PLI and a 90% reduction in VDI on the IEEE 118-bus DN.

A study investigates the optimal location of WTs and PV panels in the IEEE 33-bus DN using genetic algorithm (GA) and particle swarm optimizer (PSO) in order to reduce annual energy losses and VDI [9]. The active energy loss decreased from 453.84 MWh to 243.29 MWh per year. The VDI decreased from 4.29 to 0.79, and the minimum voltage improved from 0.91337 p.u. to 0.93880 p.u.

An energy management system was proposed [10] for optimizing the operation of BES in 21-bus DN supported by PV panels and WTs using a parallel PSO. The objective is to minimize energy costs purchased from the main grid while keeping voltage regulation and power balance. The parallel PSO achieved an average cost reduction of 1.63% and a significant reduction in processing time.

A study [11] investigated the optimal location of a combined heat and power (CHP) system in IEEE 84-bus DN incorporating PV panels and WTs. The study utilized PSO to determine the best allocation of the CHP system considering the indices of PLI, energy not supplied (ENS), and VSI. The findings demonstrated a 43.9% decrease in power loss, improvement of minimum voltage by 3.4%, and decrease of ENS by 80.31%.

A study investigated [12] the optimal allocation of WTs and PV panels as well as BESs in the IEEE 69-bus DN to achieve the lowest PLI and reactive power loss index (QLI). The study used a modified Manta Ray Foraging Optimizer algorithm. The study analyzed scenarios with WT alone, PV alone, and combined PV/WT with and without BESs. The results showed that integrating WT and PV together yield superior results compared with using single RES.

A study [13] utilized the Crow Search Algorithm to optimize the allocation of BESs, WTs, and PV panels in 33-bus IEEE DN to reduce flicker, power losses, and voltage deviation. Four scenarios were analyzed: (1) base case with no BESs, (2) optimal BESs placement and sizing, (3) optimal placement of BESs, WTs, and PVs with ESS sizing, and (4) optimal placement and sizing of all components. Results showed that scenario 2 reduced power losses by 39.5% and voltage deviation by 75.6%. Scenario 3 reduced power losses and flicker by 54.8% compared to the base case, and scenario 4 further reduced flicker emissions by 14.3%.

A novel hybrid optimization algorithm, combining enhanced elephant herding and Jaya algorithms [14], was proposed to optimize the placement and sizing of PV panels and BESs in a 69-bus IEEE DN. Compared to the base case, integrating PV panels and BESs reduced PLI by 69.64%, QLI by 68.62%, and yearly energy loss by 29.69%, while improving the minimal voltage from 0.9092 to 0.9769 p.u.

A study [15] proposed optimal allocation of WTs, PV RESs, and BESs in an IEEE 33-bus DN to improve voltage profile and minimize energy losses. The study modeled RES uncertainties, and BES characteristics, and formulated a new approach to balance demand and supply.

A study [16] investigated the optimal allocation of a hydrogen energy storage (HES) in IEEE 33-bus DN incorporating PV arrays as RESs to minimize PLI, QLI, and VDI using PSO algorithm.

An optimal allocation of WTs and BESs was investigated [17] in IEEE 69-bus DN to minimize total system power losses using a modified bald eagle search algorithm enhanced by incorporating the sine cosine algorithm. The results showed that integrating three WT units with BES decreased power loss by 65.3% compared to 58.5% with three WTs alone.

A study [18] explored the optimal planning of WTs and PV RESs and HESS combining BES and HES in IEEE 69 bus DN considering demand response (DR). The objective was to enhance DN stability by reducing fluctuations in voltage and net load and maximizing the lifecycle cost (LCC). The results showed that incorporating DR and optimal planning reduced net load fluctuation by 20.88% and voltage fluctuation by 27.40%, although the LCC increased by 2.79%.

A hybrid optimization algorithm [19] combining non-dominated sorting GA and PSO, determined optimal allocation of compressed air energy storages (CAESs) in IEEE 118-bus DN supported by WTs and PV panels. When compared to a system without ESS, the results showed that using CAESs decreased reliance on thermal generators by 15.0984% and overall investment/operation costs by 25.5026%.

A co-operative co-evolving PSO algorithm [20] allocation and size of hybrid static and mobile energy storage systems in a modified IEEE 33-bus DN with PV and synchronous generators. The goal was to maximize profit and minimize lost load costs during outages.

The high penetration levels of the intermittent RESs along with large variations of load in DNs lead to many challenges to the DNs such as excessive power losses, voltage deviation, and low voltage stability. One of the ways to alleviate these challenges is optimal allocation of RESs and energy storage systems. The aforementioned works related to the performance enhancement of DNs are briefly documented in Table 1.

Table 1: Comparison among the aforementioned works related to DNs enhancements.

Ref	Investigated Problem	Test System	RESs	HESS technologies	Optimization indices	Optimization Algorithm	Achieved improvements
3	Optimal HESS alloc. w/ PV & WT	IEEE 33-bus	PV, WT	GES, SC	Min LCC, VD, APL	PSO	Min. volt. ↑ ~0.02-0.04 pu. Peak APL ↓ ~0.07MW
4	Two-stage automated DN self-healing	Mod. IEEE 69-bus	-	BES, HES, EV battery	Min load shed & op. cost	Two-stage optimizer	Load shed ↓ 7.86%; Op. cost ↓ 3.77% (vs w/o storage)
5	Stochastic dispatch for 3-phase unbalance	Mod. IEEE 34-bus	-	HESS (BES, EVs, SC)	Min 3-phase imbalance, Total op. cost (incl. HESS degrad.)	Stochastic multistage dispatch	SC: Unbalance ↓ 3.27%, Cost ↓ $46.77/d. Incl. Degrad: Unbalance ↓ 3.62/d (vs no SC)
6	Energy efficiency in near-zero energy comm.	Near-zero energy DN	PV, Solar Thermal, Engine/Gen.	Thermal, BES, SC	Min primary energy consumption	Horse Herd Opt.	Primary energy cons. ↓ ~54.8%
7	Optimal loc/size/PF of biomass DGs	IEEE 69/33-bus	Biomass-based DGs (BDGs)	-	Min APL (PLI) within constraints	Capuchin Search Alg.	(Quantitative results not specified)
8	Optimal alloc. PV,	IEEE 118/33-bus	PV, WT	EV Charging Stations	Min PLI, VDI	-	33-bus: PLI↓ 27.2%, VDI ↓ 79.5%. 118-bus:

Ref	Investigated Problem	Test System	RESs	HESS technologies	Optimization indices	Optimization Algorithm	Achieved improvements
	WT, EV charging						PLI ↓ 34.2%, VDI↓ 90%
9	Optimal alloc. WT & PV	IEEE 33-bus	WT, PV	-	Min annual energy loss (AEL), VDI	GA, PSO	AEL ↓ 453. 8->243.3 MWh/yr; VDI ↓ 4.29->0.79; Min. volt. ↑ 0.913->0.939 pu
10	Energy management for BES operation	21-bus DN	PV, WT	BES	Min grid energy cost, Volt. reg., Power balance	Parallel PSO	Avg. cost ↓ 1.63%; Sig. processing time reduction
11	Optimal location of CHP w/ PV & WT	IEEE 84-bus	CHP, PV, WT	-	Min PLI, ENS; Improve VSI	PSO	Power loss ↓ 43.9%; Min. volt. ↑ 3.4%; ENS ↓ 80.31%
12	Optimal alloc. WT, PV, & BESS	IEEE 69-bus	WT, PV	BESS	Min PLI, QLI	Mod. Manta Ray Foraging Opt.	Combined PV/WT superior to single RES (Specifics not specified)
13	Optimal alloc. BESS, WTS, PVs	IEEE 33-bus	WTs, PVs	BESS	Min Flicker, Power losses, Volt. deviation	Crow Search Alg.	Scen 2: Loss↓ 39.5%, VDI ↓ 75.6%. Scen 4: Flicker further ↓ 14.3%
14	Optimal place/size PV & BESS	IEEE 69-bus	PV	BESS	Min PLI, QLI, Yearly energy loss; Improve min. volt.	Enh. Elephant Herding + Jaya)	PLI↓ 69.6%, QLI ↓ 68.6%; Yearly energy loss ↓ 29.7%; Min. volt. ↑ 0.909->0.977 pu
15	Optimal alloc. WTs, PVs, BESs (w/ uncert.)	IEEE 33-bus	WTs, PVs	BESs (w/ uncertainty)	Improve voltage profile; Min energy losses	-	-
16	Optimal alloc. HES (Hydrogen)	IEEE 33-bus	PV	HES	Min PLI, QLI, VDI	PSO	-
17	Optimal alloc. WTs & BESS	IEEE 69-bus	WTs	BESS	Min total system power losses	Mod. Bald Eagle Search (enh. SCA)	3WTs+BES: Power loss ↓ 65.3% (vs 58.5% for 3 WTs alone)
18	Optimal planning WTs, PVs, HESS w/ DR	IEEE 69-bus	WTs, PVs	HESS (BES+HES), DR	Enhance stability (↓ volt/load fluct.), Max LCC	-	Net load fluct. ↓ 20.9%; Volt. fluct. ↓ 27.4%; LCC ↑ 2.79%
19	Optimal alloc. CAESS	IEEE 118-bus	WTs, PVs	CAESS	Decr. thermal gen. reliance; Decr. invest/op costs	NSGA-II + PSO	Thermal gen. reliance↓ 15.1%; Total costs ↓ 25.5%

Ref	Investigated Problem	Test System	RESs	HESS technologies	Optimization indices	Optimization Algorithm	Achieved improvements
20	Alloc/size hybrid static & mobile ESS	Mod. IEEE 33-bus	PV, Sync. Generators	Hybrid Static & Mobile ESS	Max profit: Min lost load cost during outages	Co-op Co-evolving PSO	-

1.3 Paper contributions

- Proposing a simultaneous optimal integration of RESs and HESS involving GES and SC systems in a DN for decreasing voltage deviation and power losses as well as improving voltage stability based on a recently developed APO algorithm.
- Optimal locations, sizes, and operation of the RESs and HESS are assigned through solving the optimization problem. This is an addition to optimizing the weighting factors of the proposed optimized functions, without leaving them subject to the decision-maker's choices.
- The proposed method is conducted and validated by its application to the IEEE 33-bus DN with voltage-dependent time-varying mixed load model along with variable solar irradiance and wind speed.

1.4 Paper organization

The remainder of this paper is organized as follows: Section 2 details the modeling of system components including loads, RESs, and the proposed HESS. Section 3 formulates the multi-objective optimization problem, constraints, and the APO algorithm approach. Section 4 presents the simulation results on the IEEE 33-bus DN and provides a detailed discussion. Finally, Section 5 concludes the paper and suggests future research work.

2. Load, RESs, and HESS modelling

2.1 Load modelling

The DN load-demand profiles are supposed to demonstrate different normalized hourly trends for commercial, industrial, and residential loads of 1 p.u. peak at base 12.66 kV and 100 MVA as shown Fig. 2. The voltage-dependent time-varying load is modelled at bus k of the DN as follows:

$$P_k(t) = P_{ok}(t) \times V_k^{n_p}(t) \quad (1)$$

$$Q_k(t) = Q_{ok}(t) \times V_k^{n_q}(t) \quad (2)$$

where V_k is the voltage at the bus, P_{ok} and Q_{ok} are the active and reactive loads at the same bus but at nominal bus voltage, and n_p and n_q are the active and reactive load voltage exponents, respectively [21]. P_k and Q_k are the active and reactive powers injected at the kth bus, respectively.

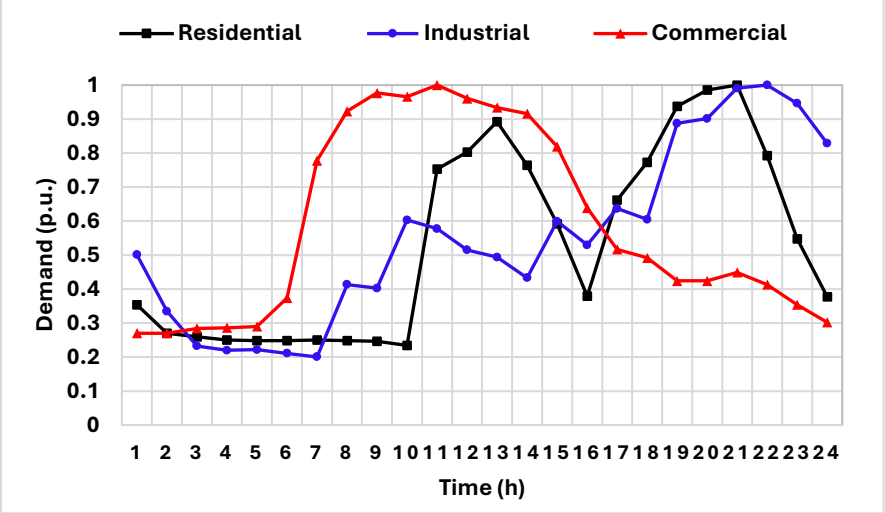

Fig. 1: Normalized hourly load demand for load models [21].

2.2 WT modeling

The power P_{WT} generated from the WT can be estimated based on wind speed v_{ws} as follows [22]:

$$P_{WT} = \begin{cases} 0 & \text{if} \quad v_{ws} < v_{ci} \; and \; v_{ws} > v_{co} \\ P_{w,r}\left(\dfrac{v_{ws} - v_{ci}}{v_{w,r} - v_{ci}}\right) & \text{if} \quad \left(v_{ci} \le v_{ws} \le v_{w,r}\right) \\ P_{w,r} & \text{if} \quad \left(v_{w,r} < v_{ws} \le v_{co}\right) \end{cases} \tag{3}$$

where $P_{w,r}$ is the rated power,$v_{w,r}$, v_{ci}, and v_{co} are the wind turbine's rated, cut-in, and cut-out wind speeds, respectively.

2.3 PV modeling

The power generated $P_{pv}(S)$ from the PV panels can be estimated based on the irradiance (S) and their rated power ($P_{pv,r}$) as follows [23]:

$$P_{pv}(\mathrm{S}) = \begin{cases} P_{pv,r}\left(\dfrac{s^2}{s_{std} \times 120}\right) & \text{if } 0 < s \le 120 \; W/m^2 \\ P_{pv,r}\left(\dfrac{s}{s_{std}}\right) & \text{if} \quad s \ge 120 \; W/m^2 \end{cases} \tag{4}$$

where s_{std} is the standard solar irradiance (1000 W/m^2) [23]. The solar irradiance and wind speed profiles over the whole day are presented in [24].

2.4 GES modeling

The construction of the GES system is illustrated in Fig. 2, which involves (i) container, (ii) wheel, (iii) suspended weight, (iv) wire rope, (v) DC machine, (vi) gearbox, (vii) power conditioning system connected with the grid. The energy storage capacity of the GES is presented as follows [25]:

$$E_{GES} = 2.78 \times 10^{-4} \times \eta_g \left(mgH_C - \frac{m^2 g}{\rho \pi r^2}\right) \tag{5}$$

where η_g is the efficiency of the GES; m, r, and ρ are the mass, radius, and density, respectively, of the suspended weight; g is the gravity acceleration; H_C is the container height, and 2.78×10^{-4} is a factor to adjust units from joule to kWh as illustrated in Fig. 2.

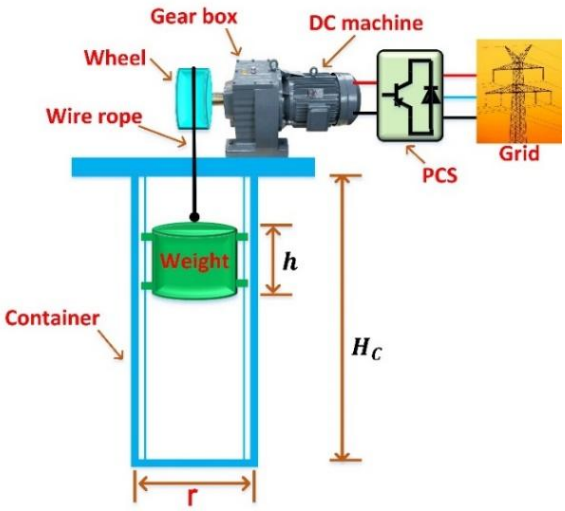

Fig. 2: Construction of GES system.

In the charging state, GES operates as a load where the suspended weight is going up [1].

$$SoC(t) = SoC(t-1) + \frac{\eta_{ch}\ \Delta t\ P_{ch}(t)}{E_{rated}} \tag{6}$$

In the discharging state, GES operates as a generator and the suspended weight is going down [1].

$$SoC(t) = SoC(t-1) - \frac{\Delta t\ P_{dis}(t)}{\eta_{dis}\ E_{rated}} \tag{7}$$

The GES present state of charge, indicated as $SoC(t)$, depends on several factors: its previous state of charge $SoC(t-1)$, the duration of charging or discharging Δt, the efficiency of the charging η_{ch} and discharging η_{dis} processes, the charging power applied $P_{ch}(t)$, and the discharging power drawn $P_{dis}(t)$. Either $P_{ch}(t)$ or $P_{dis}(t)$ equals the difference between the generated power and the load power.

2.5 SC modeling

This section models SC using Eq. (8) as follows [26]:

$$E_{SC}(t+\Delta t) = E_{SC}(t) + \eta_{sc}\ \Delta t P_{SC}(t) - \xi E_{SC}(t) \tag{8}$$

where $E_{SC}(t)$ is the energy stored in the SC at period t, η_{sc} is the charging/discharging efficiency, Δt is the time increment, P_{SC} is the power injected to (positive) or drawn from (negative) the SC, ξ is the self-discharge rate.

3. PROBLEM FORMULATION

3.1 Multi-objective function

The RESs and HESS locations and their size can be obtained optimally by minimizing the following multi-objective function:

$$MOF(t) = w_1 f_1 + w_2 f_2 + w_3 f_3 \tag{9}$$

where f_1 is the p.u. active power loss as follows [21]:

$$f_1 = \frac{\sum_{i=1}^{L} P_{Loss\ (RESs,HESS)}}{\sum_{i=1}^{L} P_{Loss\ (base\ case)}} \tag{10}$$

The "base case" refers to the DN's index value without RESs or HESSs.

f_2 is the p.u. voltage deviation as follows [21]:

$$f_2 = \frac{\sum_{i=1}^{n_b} |V_i - 1|_{(RESs,HESS)}}{\sum_{i=1}^{n_b} |V_i - 1|_{(base\ case)}} \tag{11}$$

f_3 is the p.u. voltage stability as follows [21]:

$$f_3 = \frac{\sum_{i=1}^{n_b} \left|VSI_{(k)}\right|_{(base\ case)}}{\sum_{i=1}^{n_b} \left|VSI_{(k)}\right|_{(RESs,HESS)}} \tag{12}$$

L and n_b are the number of branches and buses in DN, respectively.

w_1, w_2 and w_3 are weighting factors whose summation equals to unity. These factors are also optimized without leaving them subject to the decision-maker's choices.

The VSI is calculated as follows [21]:

$$VSI(K) = |V_i|^4 - 4(P_k \cdot X_{ik} - Q_k \cdot R_{ik})^2 - 4(P_k \cdot R_{ik} + Q_k \cdot X_{ik}) \cdot |V_i|^2 \tag{13}$$

The optimal integration of RESs and HESS for improving DN performance is determined by minimizing an average of multi-objective (*AMOF*). This *AMOF* is being obtained by averaging hourly *MOF* values over the day hours as follows:

$$AMOF(t) = \frac{1}{T} \int_0^T MOF(t)dt = \frac{1}{T} \sum_{t=1}^{T} MOF(t) \times \Delta t \tag{14}$$

The lower the *AMOF*, the more effectively the chosen placement and size of RESs and HESS in contributing to decrease of power losses, improving voltage profiles, and increase of voltage stability. The above-stated problem is solved based on a recently developed APO [1].

3.2 Problem constraints

3.2.1 Power balance constraint

The total sum of incoming and outgoing active and reactive powers flow within the analyzed DN must be balanced as follows [21]:

$$P_{Sub}(t) + \sum_{i=1}^{n_b} P_{WT,i}\,(t) + \sum_{i=1}^{n_b} P_{PV,i}\,(t) + \sum_{i=1}^{n_b} P_{SC,i}\,(t) + \sum_{i=1}^{n_b} P_{GES,i}\,(t) = \sum_{\ell=1}^{n_\ell} P_{loss,\ell}\,(t) + \sum_{i=1}^{n_b} P_{L,i}\;(t) \quad (15)$$

$$Q_{Sub}(t) = \sum_{\ell=1}^{n_\ell} Q_{loss,\ell}\,(t) + \sum_{i=1}^{n_b} Q_{L,i}\;(t) \quad (16)$$

where $P_{Sub}(t)$ and $Q_{Sub}(t)$ denote the substation active and reactive power at time t. Meanwhile, $P_{loss,\ell}(t)$ and $Q_{loss,\ell}(t)$ represent the active and reactive power losses on branch ℓ, and , $P_{L,i}(t)$ and $Q_{L,i}(t)$ correspond to the active and reactive power demands of the load at bus i.

3.2.2 Bus voltage constraint

The voltage level at every bus must be maintained within permitted limits.

$$0.95 \leq V_i(t) \leq 1.05 \quad (17)$$

3.2.3 Branch current constraint

The operating current in each branch I_ℓ must not exceed its permissible limits.

$$I_\ell(t) \leq I_{max,\ell} \quad (18)$$

3.2.4 WT constraint

$$P_{WT,min} \leq \sum_{i=1}^{n_b} P_{WT,r,i} \leq P_{WT,max} \quad (19)$$

where $P_{WT,min}$ is set to 0, and $P_{WT,max}$ is equal to the maximum active power demand.

3.2.5 PV constraint

$$P_{PV,min} \leq \sum_{i=1}^{n_b} P_{PV,r,i} \leq P_{PV,max} \quad (20)$$

where $P_{PV,min}$ is set to 0, and $P_{PV,max}$ is equal to the maximum active power demand.

3.2.6 SC constraints

$$-P_{SC,rated} \leq P_{SC}(t) \leq +P_{SC,rated} \quad (21)$$

where SC charging is indicated by positive polarity of $P_{SC,rated}$ and discharging by negative polarity.

$$E_{SC,min} \leq E_{SC}(t) \leq E_{SC,max} \quad (22)$$

where $E_{SC,min}$and $E_{SC,max}$ are considered as 0.1- and 0.9-times rated capacity ($E_{SC,rated}$) respectively.

3.2.7 GES constraints

$$-P_{GES,rated} \leq P_{GES}(t) \leq +P_{GES,rated} \quad (23)$$

where the negative and positive polarities of $P_{GES,rated}$ refers to charging and discharging of GES, respectively.

$$SOC_{GES,min} \leq SOC_{GES}(t) \leq SOC_{GES,max} \quad (24)$$

where $SOC_{GES,min}$and $SOC_{GES,max}$ are taken as 0.1 and 0.9, respectively.

4. RESULTS and DISCUSSIONS

The efficiency η_{sc} and the self-discharge rate ξ of the SC are assumed equal to 0.95 and 0.001, respectively [26]. The efficiency η_g of the GES is considered equal to 0.9 [1].
The IEEE 33 bus DN operates at 12.66 kV, comprises commercial, industrial, and residential loads supplied from a grid at the slack bus as shown in **Error! Reference source not found.** [21].

4.1 Optimal location and sizing selection

Table 2 presents the optimal locations and sizes for RESs and HESS units within the studied DN under mixed-load condition showed in Fig. 1.

Table 2: Optimized placement and capacity of RESs and HESS.

Unit type	Location (Bus #)	Size
PV	23	2108 kW
Wind	8	1500 kW
GES	23	1239 kW/ 10000 kWh
SC	8	3494 kW/ 3809 kWh

The performance of DN under mixed-load conditions is evaluated by analyzing key metrics: daily power loss, daily voltage deviation, and daily VSI.
The performance of DN under mixed-load conditions is evaluated by analyzing key metrics: daily power loss, daily voltage deviation, and daily VSI. Table 3 compares these metrics for a base case scenario with those achieved after integrating the RESs and HESS units. Significant improvements are observed in all three indices, where the daily power loss is reduced by *46.1%* against the decrease of daily voltage deviation by *64.7*%, and increase of the VSI by 7.*42*%. as shown in Fig. 3. All of this confirms that the system operates more efficiently and reliably under optimized conditions with the integrated RESs and HESS.

Table 3: Performance metrics of the DN for the base case and after installation of RESs and HESS.

Index	Base case	After	Change (%)

Daily PLI (kWh)	1418.6	764.53	- 46.1 % Reduction
Daily VDI	19.95	7.042	- 64.7 % Reduction
Daily VSI	689.34	740.48	+ 7.42 % Increase

Table 4 shows the optimized weight factors and the average value of the *AMOF* for the time-varying mixed load model. As expected, the voltage deviation index receives the highest weighting, reflecting the importance of maintaining voltage at levels to avoid sags and swells at all system buses.

Table 4: AMOF and the ideal weight factor for a mixed load model

Weight factors			*AMOF*
w_1	w_2	w_3	
0.2	0.7	0.1	0.4489

Based on the optimal sizing and availability of standard RESs, specific PV panel and WT were selected using manufacturer catalogues [27], [28]. The key operational parameters of these chosen RESs are summarized in Table 5 and form the basis for the subsequent performance evaluation.

Table 5: Parameters of the RESs.

Acciona AW-70/1500 WT				**78HL4-BDV 625–650-Watt PV panel**		
Parameter	**Unit**	**Value**		**Parameter**	**Unit**	**Value**
Rated power	MW	1.5		Standard solar irradiance	W/m^2	1000
Cut-in wind speed	m/s	4		Rated power	W	650
Rated wind speed	m/s	11.6		O.C. voltage	V	57.6
Cut-out wind speed	m/s	25		S.C. current	A	14.1
Rotor diameter	m	70		Operating voltage	V	48.33
Swept area	m^2	3848		Operating current	A	13.45
Number of blades		3		Number of cells		156 (2*78)
Gear bow type		Spur/planetary		Panel efficiency	%	23.25
Gear box ratio		1:59		Weight	kg	34
Generator type		Double fed asyn.		Dimensions	mm	2465*1134*30

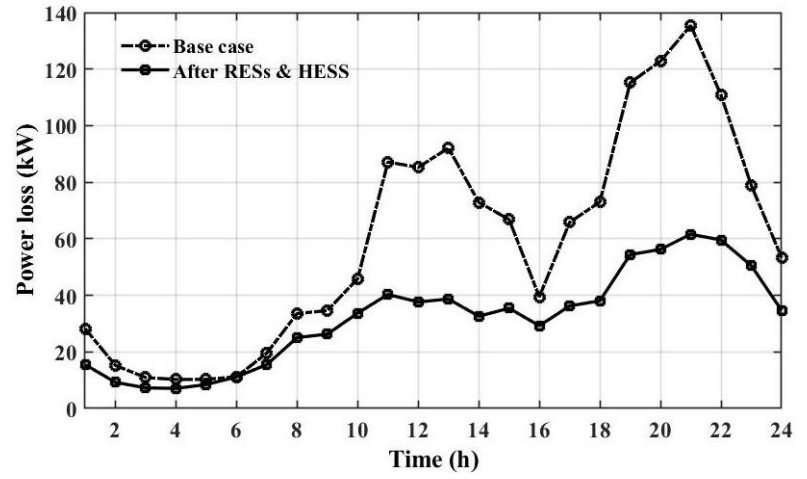

(a)

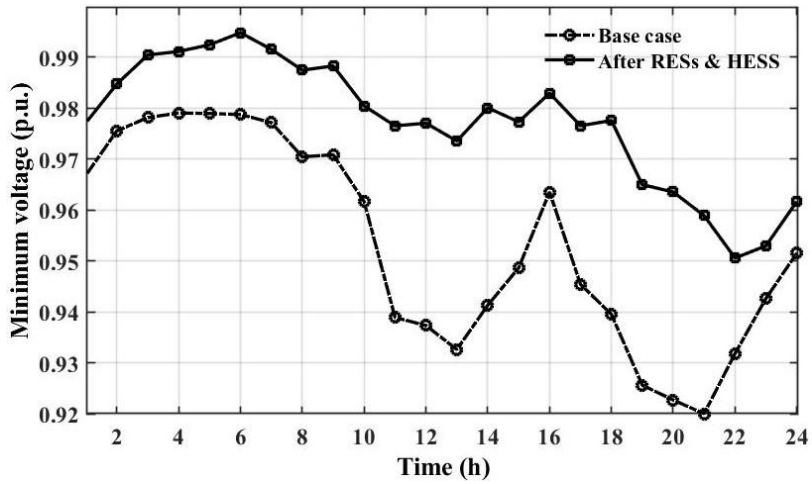

(b)

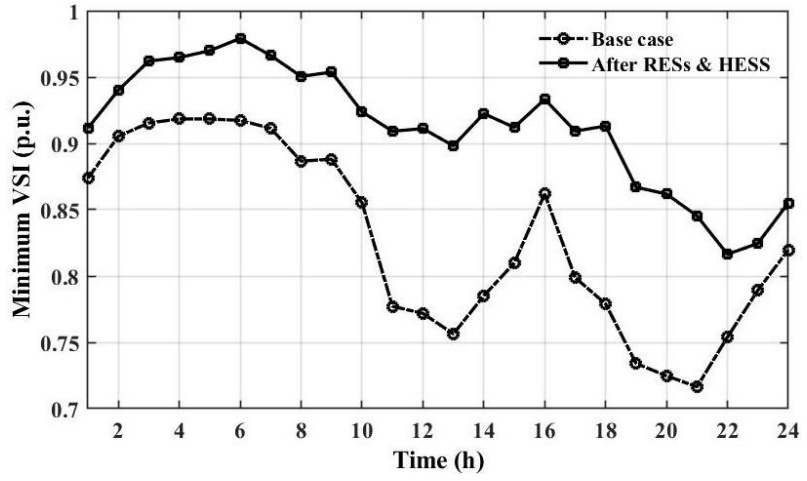

(c)

Fig. 3: System behavior metrics: (a) Power loss, (b) Minimum voltage at bus #18, and (c) Minimum VSI across a day.

4.2 State-of-charge analysis

The operation of the GES is demonstrated in Fig. 4. The SC is charged during the periods of 7-16 hrs., and is discharged during the period 17-22 hrs. The initial SOC of the supercapacitor is 0.1, rising to approximately 0.6 during its charging period, before finally being depleted

again. The peak values of charging and discharging power of the GES are 1250 and -970 kW, respectively.

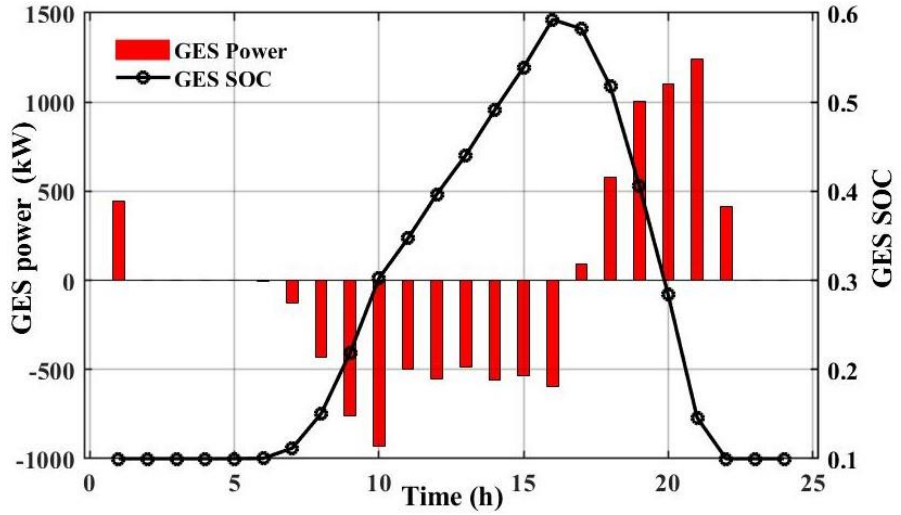

Fig. 4: Exchanged power and SOC of the GES.

The operation of the SC is demonstrated in Fig. 5. The SC is charged during the periods of 7-16 hrs., and is discharged during the period 17-22 hrs. The initial SOC of the supercapacitor is 0.1, rising to approximately 0.65 during its charging period, before finally being depleted again. The peak values of charging and discharging power of the SC are 564 and -397 kW, respectively.

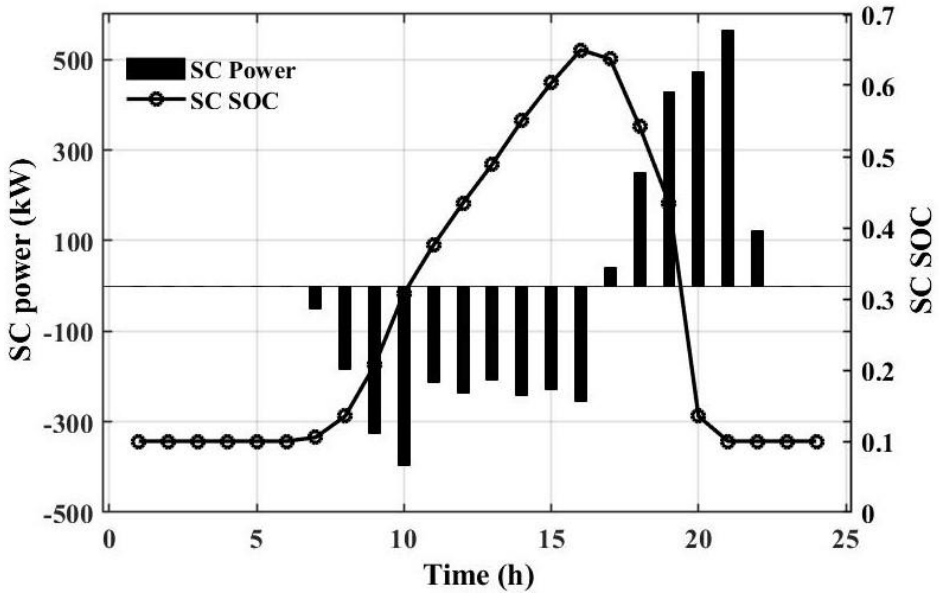

Fig. 5: Exchanged power and SOC of the SC.

5. Conclusions and future work

Due to the high penetration levels of the intermittent RESs along with large variations of load in DNs lead to numerous challenges to the DN such as excessive power losses, voltage deviation, and low voltage stability. This present research study addressed the challenges and improved the steady-state performance of the DN through optimal integration of RESs and HESS. The main contributions of the present work are summarized as follows:

- A novel optimization method called APO algorithm is introduced to find the best allocation and operation of RESs and HESS within a DN.
- The optimization method simultaneously targets multiple goals including minimizing voltage deviations and power losses while enhancing voltage stability in DN.
- The method eliminates arbitrary weight factor selection by automatically optimizing these values, resulting in voltage deviation objective to assume the highest weight.
- The proposed method for optimal allocation and operation of RES and HESS is successfully tested using the IEEE 33-bus DN, which includes variations in load, wind speed, and solar irradiance.
- The method successfully minimizes power loss by 46.1 % and voltage deviation by 64.7 %, as well as improve voltage stability by 7.42 %, leading to a significant improvement in the overall DN performance.
- The limitation of this study is that considering the optimization problem investigated on a small-scale IEEE 33-bus DN.
- Future work will enhance the DN performance more by introducing additional indices such as reliability and security on seeking the optimal allocation of RESs and HESS.

References

[1] M. El-Ghazaly, M. Abdel-Salam, M. Nayel, and M. Hashem, “Techno-economic utilization of hybrid optimized gravity-supercapacitor energy-storage system for enriching the stability of grid-connected renewable energy sources,” *J Energy Storage*, vol. 107, no. December 2024, p. 115002, 2025, Doi: 10.1016/j.est.2024.115002.

[2] M. Khamies, M. Abdel-Salam, A. Kassem, M. Nayel, M. El-Ghazaly, and M. Hashem, “Evaluating supercapacitor energy storage for voltage sag minimization in a real distribution feeder,” *J Energy Storage*, vol. 101, no. PA, p. 113742, 2024, Doi: 10.1016/j.est.2024.113742.

[3] X. F. Xu *et al.*, “multi-objective particle swarm optimization algorithm based on multi-strategy improvement for hybrid energy storage optimization configuration,” *Renew Energy*, vol. 223, p. 120086, 2024, Doi: 10.1016/j.renene.2024.120086.

[4] S. Nourian and A. Kazemi, “A two-stage optimization technique for automated distribution systems self-healing: Leveraging internet data centers, power-to-hydrogen units, and energy storage systems,” *J Energy Storage*, vol. 85, no. November, p. 111084, 2024, Doi: 10.1016/j.est.2024.111084.

[5] S. Zhou, Y. Han, A. S. Zalhaf, M. Lehtonen, M. M. F. Darwish, and K. Mahmoud, “A novel stochastic multistage dispatching model of hybrid battery-electric vehicle-supercapacitor storage system to minimize three-phase unbalance,” *Energy*, vol. 296, no. December, p. 131174, 2024, Doi: 10.1016/j.energy.2024.131174.

[6] L. Meng, M. Li, and H. Yang, “Enhancing energy efficiency in distributed systems with hybrid energy storage,” *Energy*, vol. 305, p. 132197, 2024, Doi: 10.1016/j.energy.2024.132197.

[7] A. Fathy, D. Yousri, H. Rezk, and H. S. Ramadan, “An efficient capuchin search algorithm for allocating the renewable based biomass distributed generators in radial distribution network,”

Sustainable Energy Technologies and Assessments, vol. 53, no. PB, p. 102559, 2022, Doi: 10.1016/j.seta.2022.102559.

[8] K. E. Adetunji, I. W. Hofsajer, A. M. Abu-mahfouz, and L. Cheng, "An optimization planning framework for allocating multiple distributed energy resources and electric vehicle charging stations in distribution," *Appl Energy*, vol. 322, no. December 2021, p. 119513, 2022, Doi: 10.1016/j.apenergy.2022.119513.

[9] M. Purlu and B. E. Turkay, "Optimal Allocation of Renewable Distributed Generations Using Heuristic Methods to Minimize Annual Energy Losses and Voltage Deviation Index," *IEEE Access*, vol. 10, pp. 21455–21474, 2022, Doi: 10.1109/ACCESS.2022.3153042.

[10] L. F. Grisales-Noreña, O. D. Montoya, and C. A. Ramos-Paja, "An energy management system for optimal operation of BSS in DC distributed generation environments based on a parallel PSO algorithm," *J Energy Storage*, vol. 29, no. April, p. 101488, 2020, Doi: 10.1016/). The.2020.101488.

[11] A. Naderipour, Z. Abdul-Malek, S. A. Nowdeh, V. K. Ramachandaramurthy, A. Kalam, and J. M. Guerrero, "Optimal allocation for combined heat and power system with respect to maximum allowable capacity for reduced losses and improved voltage profile and reliability of microgrids considering loading condition," *Energy*, vol. 196, p. 117124, 2020, Doi: 10.1016/j.energy.2020.117124.

[12] H. Abdel-Mawgoud, A. Ali, S. Kamel, C. Rahmann, and A. M. M. A., "A Modified Manta Ray Foraging Optimizer for Planning Inverter-Based Photovoltaic with Battery Energy Storage System and Wind Turbine in Distribution Networks," *IEEE Access*, vol. 9, pp. 91062–91079, 2021, Doi: 10.1109/ACCESS.2021.3092145.

[13] A. Ghaffari, A. Askarzadeh, and R. Fadaeinedjad, "Optimal allocation of energy storage systems, wind turbines and photovoltaic systems in distribution network considering flicker mitigation," *Appl Energy*, vol. 319, no. February, p. 119253, 2022, Doi: 10.1016/j.apenergy.2022.119253.

[14] S. Pemmada, N. R. Patne, A. D. Manchalwar, and R. Panigrahi, "A novel hybrid algorithm based optimal planning of solar PV and battery energy storage systems," *Energy Reports*, vol. 9, pp. 380–387, 2023, Doi: 10.1016/j.egyr.2023.05.157.

[15] O. Khoubseresht, M. Rajabinezhad, and S. Y. Mousazadeh Mousavi, "An analytical optimum method for simultaneous integration of PV, wind turbine and BESS to maximize technical benefits," *IET Generation, Transmission and Distribution*, vol. 17, no. 10, pp. 2207–2227, 2023, Doi: 10.1049/gtd2.12801.

[16] R. A. Ufa, Y. Y. Malkova, Y. D. Bay, and A. V. Kievets, "Analysis of the problem of optimal placement and capacity of the hydrogen energy storage system in the power system," *Int J Hydrogen Energy*, vol. 48, no. 12, pp. 4665–4675, 2023, Doi: 10.1016/j.ijhydene.2022.10.221.

[17] S. Kamel, H. Abdel-Mawgoud, M. M. Alrashed, L. Nasrat, and M. F. Elnaggar, "Optimal allocation of a wind turbine and battery energy storage systems in distribution networks based on the modified BES-optimizer," *Front Energy Res*, vol. 11, no. January, pp. 1–15, 2023, Doi: 10.3389/fenrg.2023.1100456.

[18] J. Li *et al.*, "Optimal planning of Electricity–Hydrogen hybrid energy storage system considering demand response in active distribution network," *Energy*, vol. 273, no. December 2022, p. 127142, 2023, Doi: 10.1016/j.energy.2023.127142.

[19] A. K. ALAhmad, R. Verayiah, A. Ramasamy, M. Marsadek, and H. Shareef, "Optimal planning of energy storage system for hybrid power system considering multi correlated input stochastic variables," *J Energy Storage*, vol. 82, no. December 2023, p. 110615, 2024, Doi: 10.1016/j.est.2024.110615.

[20] P. K. Ganivada, T. H. M. El-Fouly, H. H. Zeineldin, and A. Al-Durra, "Optimal siting and sizing of mobile-static storage mix in distribution systems with high renewable energy resources penetration," *Electric Power Systems Research*, vol. 226, no. October 2023, p. 109860, 2024, Doi: 10.1016/j.epsr.2023.109860.

[21] M. Hashem, M. Abdel-Salam, M. T. El-Mohandes, M. Nayel, and M. Ebeed, "Optimal Placement and Sizing of Wind Turbine Generators and Superconducting Magnetic Energy Storages in a Distribution System," *J Energy Storage*, vol. 38, p. 102497, Jun. 2021, Doi: 10.1016/J.EST.2021.102497.

[22] A. T. Hachemi, R. M. Kamel, M. Hashem, M. Ebeed, and A. Saim, "Reliability and line loading enhancement of distribution systems using optimal integration of renewable energy and compressed air

energy storages simultaneously under uncertainty," *J Energy Storage*, vol. 101, no. PB, p. 113921, 2024, Doi: 10.1016/j.est.2024.113921.

[23] P. P. Biswas, P. N. Suganthan, R. Mallipeddi, and G. A. J. Amaratunga, "Optimal reactive power dispatch with uncertainties in load demand and renewable energy sources adopting scenario-based approach," *Applied Soft Computing Journal*, vol. 75, pp. 616–632, 2019, Doi: 10.1016/j.asoc.2018.11.042.

[24] A. El-Zonkoly, "Application of smart grid specifications to overcome excessive load shedding in Alexandria, Egypt," *Electric Power Systems Research*, vol. 124, pp. 18–32, 2015, Doi: 10.1016/j.epsr.2015.02.019.

[25] A. Rathore and N. P. Patidar, "Optimal sizing and allocation of renewable based distribution generation with gravity energy storage considering stochastic nature using particle swarm optimization in radial distribution network," *J Energy Storage*, vol. 35, no. October 2020, p. 102282, 2021, Doi: 10.1016/j.est.2021.102282.

[26] A. F. Güven, S. Kamel, and M. H. Hassan, *Optimization of grid-connected photovoltaic/wind/battery/supercapacitor systems using a hybrid artificial gorilla troops optimizer with a quadratic interpolation algorithm*, vol. 0123456789. 2024. Doi: 10.1007/s00521-024-10742-w.

[27] "wind-turbine." [Online]. Available: https://en.wind-turbine-models.com/turbines/777-acciona-aw-70-1500

[28] "Jinko Solar Panel." [Online]. Available: https://www.jinkoja.com/product-item-39.html